International Journal on Emerging Technologies **10**(2): 455-461(2019)

**ISSN No. (Print) : 0975-8364**
**ISSN No. (Online) : 2249-3255**

# A Method for Diagnosis of Tuberculosis using Combined Blur and Affine Moment Invariants on Cavity Image

***K. Durga Prasad[1] and M.B.R Murthy[2]***
*[1]Research Scholar, Department of Electronics and Communication Engineering, Rayalaseema University – Kurnool, Andhra Pradesh, India.*
*[2]Adjunct Professor, Department of Electronics and Communication Engineering, RGUKT (IIIT) Basara, Telangana, India.*

*(Corresponding author: K. Durga Prasad)*
*(Received 31 May 2019, Revised 17 August 2019 Accepted 28 August 2019)*
*(Published by Research Trend, Website: www.researchtrend.net)*

**ABSTRACT: In the entire World 1/3 of people are infected with TB, which is caused by mycobacterium Tuberculosis Bacteria and for every second one infection case is recording. The first attack of tuberculin bacterium in the Human body is on Lungs that can be indicated by small damaging portions called cavities. The intensity of TB infection is estimated by number of cavities and size of the cavity areas on lungs. Generally, the area of cavity has been detected by physician to know the effect of TB. In this paper a new automatic technique proposed for fast and accurate detection of TB disease with Computer-Aided Diagnosis (CAD) system using combine blur and affine moment Invariants (CBAMI). The CAD method not only provides second opinion to radiologist, but also accelerates the process of active case finding. This method consists of three major steps (1) image pre-processing (2) feature extraction (3) classification. The CBAMI are selected as features in this paper because they are invariant to both affine distortions as well as blur. The CBAMI features are applied on cavity segmented Tuberculosis chest X-Ray image and local threshold used as classifier.**

**Keywords:** Tuberculosis, Computer Aided Diagnosis, Cavity Extraction, Combined Blur and Affine Moment Invariants, Lungs segmentation.

**Abbreviations:** *CBAMI-Combined blur and affine moment invariants,* TB – Tuberculosis, CAD - Computer Aided Diagnosis, CXR - chest radiography

## I. INTRODUCTION

Tuberculosis (TB) is a major public health problem, it's a worldwide health threat. The TB is an infectious disease caused by bacillus mycobacterium tuberculosis. It affects the lung (pulmonary TB) portions. It is a communication disease [1] which spreads through coughing and sneezing of the infected person. If the person is living with HIV, the probability to attach TB disease is very high. The most efficient solution for prevention of this disease is to detect its presence as early as possible in the affected person. There are different methods available for screening of TB namely (i) The Sputum smear microscopy (ii)Tuberculin skin test iii) Rapid molecular test and (iv) Chest radiography test. Sputum smear microscopy is a screening method in which sputum samples are examined under a microscope to see if bacteria are present or not. Its sensitivity is reduced in patients with HIV co-infection[2].In Tuberculin skin test, a small amount of tuberculin is injected into the skin and the size of swelling is observed. This method is not reliable as it causes misclassification [1]. Latest rapid molecular tests are fast and accurate. But, their availabilities and cost is a big primary concerned. The HU recommended chest radiography (CXR) for screening proposes for early detection of TB. Early detection leads to success of anti TB therapy. It also helps to control over transmission of infection as well as development of drug resistant TB.

Moments are the projections of image intensities, these can be applied to different aspects of image processing operations. Moments are used in military photo interpretation, pattern recognition and many applications in digital Image processing. A set of six moment invariants which were derived by John Flusser from geometrical moments, these moments are invariant to affine distortions as well as blurring of the image, they are called as Combined blur and affine moment invariants (CBAMI). These are used for recognizing objects in the degraded scene. The CBAMI equations are invariant to translation, rotation, scaling, affine distortions and noise.

Especially in developing countries, because of lack of skilled radiologists and other resources, it becomes difficult for effective diagnosis. Hence, Computer Aided Diagnosis (CAD) tool can gain lot of significance because they not only reduce diagnostic errors but also increases the efficiency of mass screening in poor resource setting. CAD method provides second opinion to the radiologists for their finding. It provides better diagnosis of cancer and other diseases including TB.

## II. LITERATURE REVIEW

In the literature, for object recognition applications, Histogram of Oriented Gradients (HOG) are used as

features. Sivaranjani [6] proposed a method for analysis of TB with HOG as features and SVM as classifier. Ankitha *et al* [7] proposed a method to extract the lung field by an interactive lung field segmentation based on active contour models. After segmentation process, they analyzed the pixel data within region of interest using first order statistics to extract textural properties in classifying image as TB and non TB.A method using HOG Features in Computer-Aided Diagnosis of Tuberculosis without Segmentation was proposed in [8]. Pallavi *et al.* [9] used first order statistical properties such as mean and entropy for diagnosis of TB.

Hu [10] introduced geometric moments based on monomials. He derived a set of seven moment invariants which are invariant with respect to change in image translation, rotation and scale. Flusser *et al* [11] derived blur invariants which are invariant with respect to blurring on the acquired image. Blur invariants are required because real imaging systems as well as imaging conditions are imperfect. Blur may occur in the captured image during the image acquisition process because of the factors such as lane aberration, diffraction, wrong focus and atmospheric turbulence. They proposed an approach which describes images by features that are invariant with respect to blur and recognize images in the feature space. In order to obtain features which are invariant to blur as well as affine distortion, Suk and Flusser [12] derived combined blur and affine moment invariants. Combined invariants are capable of recognizing objects in the degraded scene without any restoration.

Most of the methods discussed above for diagnosis of Tuberculosis is based on histogram of oriented features, calculation of mean, variance, third moment and entropy features as well Geometric moment invariants. All these methods do not take care into account of blur as well as affine distortion present in the Tb X-ray image. In order to solve this problem and to obtain better accuracy, we propose an efficient method for detection of Tuberculosis in this Paper. The proposed method computes Combined Blur and Affine Moment Invariants (CBAMI) on X-ray image and uses them as feature for detection of tuberculosis.

In order to solve this problem and to obtain better accuracy, we propose an efficient method for detection of Tuberculosis in this Paper.

The proposed method computes Combined Blur and Affine Moment Invariants (CBAMI) on X-ray image and uses them as feature for detection of tuberculosis. The CBAMI features are applied on entire X-Ray image for the detect Tuberculosis the accuracy is 88%.

In the second step Combined Blur and Affine Moment Invariants (CBAMI) are computed on cavity segmented X-ray image and uses them as feature for detection of tuberculosis. The CBAMI features are applied on cavity segmented X-Ray image for the detect Tuberculosis the accuracy is 96%.

In this paper TB detection process consists of following steps: (i) Preprocessing, such as resizing, smoothing of image using median filter. (ii) Lungs segmentation. (iii) Cavities extraction. (iv) computation of CBAMI features. (v) Euclidean distance computation is used for classification of images. The last section presents the conclusions about the work.

## III. MOMENT INVARIANT EQUATIONS

In this section, we present details about Geometric, moments, Geometric Moment Invariants and Combined Blur and Affine Moment Invariants.

### *A. Geometric Moments and their Invariants*

The Geometric moments of order (p, q) for an image $f(x,y)$ are defined [10] as

$$M_{pq} = \int_{-\infty}^{\infty}\int_{-\infty}^{\infty} x^p\, y^q\, f(x,y)\, dx\, dy \qquad (1)$$

where $p,q = 0,1,2,.....,\infty$

To keep the dynamic range of $M_{pq}$ consistent for different size images, the N x M image plane is first mapped onto a square defined by $x \in [-1,+1],\ y \in [-1,+1]$ . Then $M_{pq}$ can be written as

$$M_{pq} = \int_{-1}^{1}\int_{-1}^{1} x^p\, y^q\, f(x,y)\, dx\, dy \qquad (2)$$

The discrete form representation of the above expression is given by

$$M_{pq} = \sum_{i=0}^{N-1}\sum_{j=0}^{M-1} x_i^p\, y_j^q\, f(x_i, y_j)\, \Delta x \Delta y \qquad (3)$$

where $(x_i, y_j)$ is the centre of (i, j) pixel and $\Delta x = x_i - x_{i-1}$ , $\Delta y = y_j - y_{j-1}$ are the sampling intervals in the 'x' and 'y' directions respectively. N x M corresponds to the size of the image.

The Geometric central moments [10] are defined as

$$\mu_{pq} = \int_{-\infty}^{\infty}\int_{-\infty}^{\infty} (x-\bar{x})^p\ (y-\bar{y})^q f(x,y)\, dx\, dy \qquad (4)$$

where $\bar{x} = \frac{M_{10}}{M_{00}}$ and $\bar{y} = \frac{M_{01}}{M_{00}}$ (5)

For a digital image, the Geometric central moments can be written as

$$\mu_{pq} = \sum_{i=0}^{N-1}\sum_{j=0}^{M-1} (x_i - \bar{x})^p\, (y_j - \bar{y})^q\, f(x_i, y_j)\, \Delta x \Delta y \qquad (6)$$

The normalized central moments [10] are defined as

$$\eta_{pq} = \frac{\mu_{pq}}{\mu_{00}^{\gamma}} \qquad (7)$$

where $\gamma = \frac{p+q}{2} + 1$ for $p + q = 2,3,.....$

### *B. Combined Blur and Affine Moment Invariants*

Jan Flusser *et al.* [12] derived combined blur and affine moment invariants. Combined invariants are capable of recognizing objects in the degraded scene without any restoration. The Combined Blur and Affine Moment Invariants (CBAMI) are given below

$Set_1 = \mu^2_{30}\,\mu^2_{03} - 6\,\mu_{30}\,\mu_{21}\,\mu_{12}\,\mu_{03} + 4\,\mu_{30}\,\mu^3_{12} + 4\,\mu^3_{21}\,\mu_{03} - 3\,\mu^2_{21}\,\mu^2_{12})/\,\mu^{10}_{00}.$ (8)

$Set_2 = \mu^2_{50}\,\mu^2_{05} - 10\,\mu_{50}\,\mu_{41}\,\mu_{14}\,\mu_{05} + 4\,\mu_{50}\,\mu_{32}\,\mu_{23}\,\mu_{05} + 16\,\mu_{50}\,\mu_{32}\,\mu^2_{14} - 12\,\mu_{50}\,\mu_{14}\,\mu^2_{23} + 16\,\mu^2_{41}\,\mu_{23}\,\mu_{05} + 9\,\mu^2_{41}\,\mu^2_{14} - 12\,\mu_{41}\,\mu^2_{32}\,\mu_{05} - 72\,\mu_{32}\,\mu_{41}\,\mu_{14}\,\mu_{23} + 48\,\mu^3_{23}\,\mu_{41} + 48\,\mu_{14}\,\mu^3_{32} - 32\,\mu^2_{32}\,\mu^2_{23})\,/\,\mu^{14}_{00}.$ (9)

$Set_3 = (\mu^2_{30}\mu_{05}\,\mu_{12} - \mu^2_{30}\mu_{03}\,\mu_{14} - \mu_{30}\mu^2_{21}\,\mu_{05} - 2\,\mu_{30}\,\mu_{21}\,\mu_{12}\,\mu_{14} + 4\,\mu_{30}\,\mu_{21}\,\mu_{23}\,\mu_{03} + 2\,\mu_{30}\mu^2_{12}\,\mu_{23} - 4\,\mu_{30}\,\mu_{12}\,\mu_{32}\,\mu_{03} + \mu_{30}\mu^2_{03}\,\mu_{41} + 3\,\mu^3_{21}\,\mu_{14} - 6\,\mu^2_{21}\mu_{12}\,\mu_{23} - 2\,\mu^2_{21}\mu_{03}\,\mu_{32} + 6\,\mu_{21}\mu^2_{12}\,\mu_{32} + 2\,\mu_{12}\,\mu_{21}\,\mu_{41}\,\mu_{03} - \mu_{21}\mu^2_{03}\,\mu_{50} - 3\,\mu^3_{12}\,\mu_{41} + \mu^2_{12}\mu_{03}\,\mu_{50})\,/\,\mu^{11}_{00}.$ (10)

$Set_4 = (2\,\mu_{30}\,\mu_{12}\,\mu_{41}\,\mu_{05} - 8\,\mu_{30}\,\mu_{12}\,\mu_{32}\,\mu_{14} + 6\,\mu_{30}\,\mu_{12}\,\mu^2_{23} - \mu_{30}\,\mu_{03}\,\mu_{50}\,\mu_{05} + 3\,\mu_{30}\,\mu_{03}\,\mu_{41}\,\mu_{14} - 2\,\mu_{30}\,\mu_{03}\,\mu_{23}\,\mu_{32} - 2\,\mu^2_{21}\mu_{41}\,\mu_{05} + 8\,\mu^2_{21}\mu_{32}\,\mu_{14} - 6\,\mu^2_{21}\,\mu^2_{23} + \mu_{21}\,\mu_{12}\,\mu_{50}\,\mu_{05} - 3\,\mu_{21}\,\mu_{12}\,\mu_{41}\,\mu_{14} + 2\,\mu_{21}\,\mu_{12}\,\mu_{32}\,\mu_{23} + 2\,\mu_{21}\,\mu_{03}\,\mu_{50}\,\mu_{14} - 8\,\mu_{21}\,\mu_{03}\,\mu_{41}\,\mu_{23} + 6\,\mu_{21}\,\mu_{03}\,\mu^2_{32} - 2\,\mu^2_{12}\mu_{50}\,\mu_{14} + 8\,\mu^2_{12}\mu_{41}\,\mu_{23} - 6\,\mu^2_{12}\,\mu^2_{32})\,/\,\mu^{12}_{00}.$ (11)

$Set_5 = (\mu_{30}\,\mu_{41}\,\mu_{23}\,\mu_{05} - \mu_{30}\,\mu_{41}\,\mu^2_{14} - \mu_{30}\mu^2_{32}\,\mu_{05} + 2\,\mu_{30}\,\mu_{32}\,\mu_{23}\,\mu_{14} - \mu_{30}\,\mu^3_{23} - \mu_{21}\,\mu_{50}\,\mu_{23}\,\mu_{05} + \mu_{21}\,\mu_{50}\,\mu^2_{14} + \mu_{21}\,\mu_{41}\,\mu_{32}\,\mu_{05} - \mu_{21}\,\mu_{41}\,\mu_{23}\,\mu_{14} - \mu_{21}\mu^2_{32}\,\mu_{14} + \mu_{21}\,\mu_{32}\,\mu^2_{23} + \mu_{12}\,\mu_{50}\,\mu_{32}\,\mu_{05} - \mu_{12}\,\mu_{50}\,\mu_{23}\,\mu_{14} - \mu_{12}\mu^2_{41}\,\mu_{05} + \mu_{12}\,\mu_{41}\,\mu_{32}\,\mu_{14} + \mu_{12}\,\mu_{41}\,\mu^2_{23} - \mu_{12}\mu^2_{32}\,\mu_{23} - \mu_{03}\,\mu_{50}\,\mu_{32}\,\mu_{14} + \mu_{03}\,\mu_{50}\,\mu^2_{23} + \mu_{03}\mu^2_{41}\,\mu_{14} - 2\,\mu_{03}\,\mu_{41}\,\mu_{23}\,\mu_{32} + \mu_{03}\,\mu^3_{32})\,/\,\mu^{13}_{00}.$ (12)

$Set_6 = (\mu^2_{70}\,\mu^2_{07} - 14\,\mu_{70}\,\mu_{61}\,\mu_{16}\,\mu_{07} + 18\,\mu_{70}\,\mu_{52}\,\mu_{25}\,\mu_{07} + 24\,\mu_{70}\,\mu_{52}\,\mu^2_{16} - 10\,\mu_{70}\,\mu_{43}\,\mu_{34}\,\mu_{07} - 60\,\mu_{70}\,\mu_{43}\,\mu_{25}\,\mu_{16} - 234\,\mu_{61}\,\mu_{52}\,\mu_{25}\,\mu_{16} + 40\,\mu_{61}\mu^2_{43}\,\mu_{07} + 50\,\mu_{61}\,\mu_{43}\,\mu_{34}\,\mu_{16} + 360\,\mu_{61}\,\mu_{43}\,\mu^2_{25} - 240\,\mu_{61}\mu^2_{34}\,\mu_{25} + 360\,\mu^2_{52}\mu_{34}\,\mu_{16} + 81\,\mu^2_{52}\,\mu^2_{25} - 240\,\mu_{52}\mu^2_{43}\,\mu_{16} - 990\,\mu_{52}\,\mu_{43}\,\mu_{34}\,\mu_{25} + 600\mu_{52}\,\mu^3_{34} + 600\mu^3_{43}\,\mu_{25} - 375\,\mu^2_{43}\,\mu^2_{34})\,/\,\mu^{18}_{00}.$ (13)

## IV. PROPOSED METHOD

The proposed technique for detection of TB is shown in Fig.1.

The first step is used to resize the image and remove background noise. In this work, we used median filtering for smoothing. The Captured X-Ray image contains large amount of unwanted regions such as background region, bones and unaffected muscle areas. The Captured X-Ray image converted into cavity image for avoiding unwanted regions. Combine blur and affine moment invariants are computed on cavity image. Combine blur and affine moment invariants are selected as features because they are invariant with respect to image blur and affine distortions. In presence of these distortions also, the computed features are invariants. The extracted features are then applied on cavity images for classification with and without TB features using Euclidean distance classifier. The results are carried out by comparing X-ray image and cavities segmented Images using CBAMI method. In X-Ray image there is a unwanted regions which are not affected by the TB are eliminated and only cavity regions are extracted. The CBAMI method gives more accuracy with cavity extracted image than entire X-Ray image.

Processing steps

(i) Preprocessing, such as resizing, smoothing of image using median filter.
(ii) Histogram equalization
(iii) Lungs segmentation.
(iv) Cavities extraction.
(v) Computation of CBAMI features.
(vi) Euclidean distance computation with and without TB features.

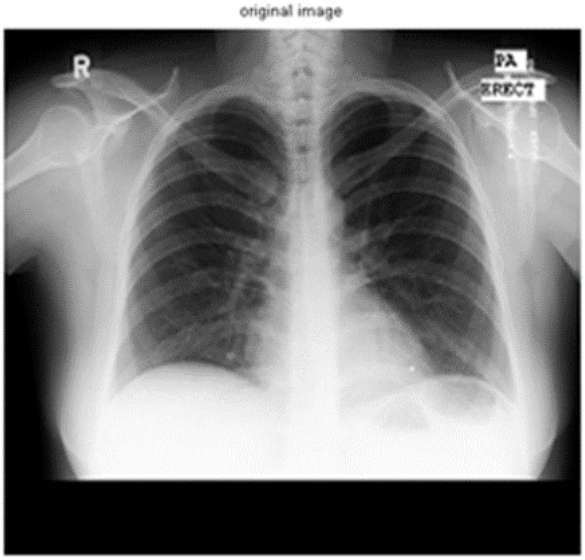


**Fig. 1.** TB Image.

Preprocessing is a common operation on captured images, both input and output are intensity images. The main objective of pre-processing is an improvement in the image data that suppresses unnecessary distortions such as noise and enhances image features which are essential for further processing.

**Image Resize:** The captured image is either 4,020x4,892 or 4,892x4,020 pixels. These images are resized to 450 x 450 pixels. Resizing of X-Ray image is important because large size image contains large number of pixels that leads to increase computational time, hence we have to reduce size of the image. If the image size is too small, there is insufficient number of pixels in the image to find features of the image.

The unwanted electrical fluctuations in signals introduced in a image at the time of image capturing is called noise. Noise is random variation of brightness in images, it is a disagreeable by-product of image capture that obscures the desired information. After resizing the captured image, noise in the image is removed by using median filter.

A histogram is a gray scale image graph provides a graphic interpretation of numerical data by indicating the number of data points that lie within a range of values. In our research work histogram used to recognize the threshold range for black & white intensity value.

Convert the X-Ray image into black and white binary image. Set threshold range in such a way that, which works best to display the image with better intensity difference. Fill small structuring regions with white spots and remove small gaps. Calculate areas for all white regions from the filtered image, the white regions which will probably fit within the area range of a cavity.

The set of six CBAMI features (equations no.8 to 13) are applied on cavity extracted images for both Reference (Non-TB) image and Test image (TB image).Euclidean distance computed for with and without TB features.

The Euclidean distance between Non-TB image and Test image is greater than threshold value then the Test image is TB Image. If the Euclidean distance between Non-TB image and Test image is less than threshold value then the Test image is TB free Image.
Local Threshold value is used as classifier for detection Tuberculosis.

## V. SIMULATION RESULTS

To test the proposed approach, we considered The Montgomery County dataset. This dataset is collected online freely from the Department of Health and Human Services, Montgomery County, Maryland, USA. It consists of 138 frontal chest X-rays from Montgomery Country Tuberculosis screening program, out of which 80 are normal cases and 58 are cases with manifestations of TB. These X-rays were captured with a Eureka stationary X-ray machine (CR), and are provided in Portable Network Graphics (PNG) format as 12-bit gray level images. The size of the X-rays is either 4,020x4,892 or 4,892x4,020 pixels. These images are resized to 450 x 450 pixels. Some of the database images are shown in figures. For testing of invariance property of CBAMI under different distortions, we selected image as shown in Fig. 2. The computed CBAMI values are entered in Table.1. From the results, it is observed that these features are invariant with respect to affine distortions such as rotation, scale and blurring.

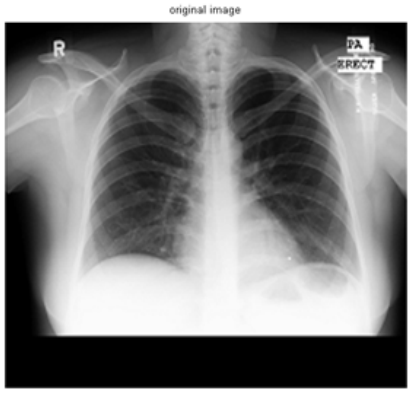


**Fig. 2.** Original Non- TB image.

**Table 1: Scaling, rotation and blurred image properties.**

| CBAMI | Non TB Image | Half size | Rotated by$20^0$ | Blurred by LPF |
|---|---|---|---|---|
| Set1 | 1.74e-22 | 1.74e-22 | 1.74e-22 | 1.74e-22 |
| Set2 | 1.58e-32 | 1.58e-32 | 1.58e-32 | 1.57e-32 |
| Set3 | 7.27e-27 | 7.29e-27 | 7.28e-27 | 7.07e-27 |
| Set4 | -1.66e-27 | -1.66e-27 | -1.66e-27 | -1.65e-27 |
| Set5 | 2.68e-32 | 2.68e-32 | 2.68e-32 | 2.73e-32 |
| Set6 | -0.03272 | -8.18e-06 | -1.75e-02 | -0.032 |

The CBAMI features are shown in Table 1.
The six CBAMI features set1 to set5 for X-Ray image are almost same for Scaling, Rotation and Bluring, for set6 is used for finding reflections in the image. Hence it is proved that CBAMI features are invariant to Scaling, Rotation and Bluring.

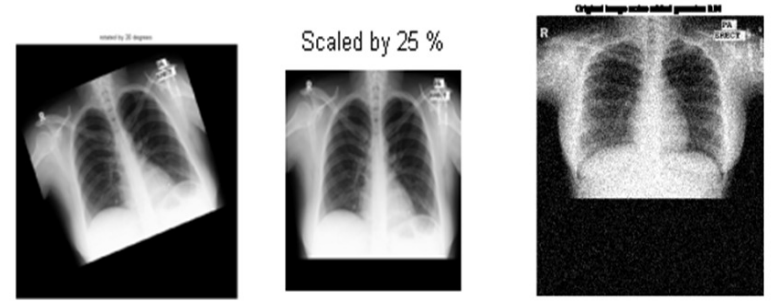


**Fig. 3.** Some Images used for Invariant properties.

**Detection of TB**
CBAMI features are computed for Non-TB X-ray image (set1 to set6) and for TB X-ray image (SET1 to SET6). The Euclidean Distance (ED) is calculated by

$$ED = \sqrt{((\text{set1} - \text{SET1})^2 + (\text{set2} - \text{SET2})^2 + (\text{set3} - \text{SET3})^2 + (\text{set4} - \text{SET4})^2 + (\text{set5} - \text{SET5})^2 + (set6 - SET6)^2}$$

The global threshold cannot give accurate results because varied intensity distribution in X-Ray images. Therefore, for X-Ray images Local threshold is needed and is determined from Image attributes(Average, Maximum, Minimum, mean etc).Local threshold can be calculated by practicing number of exercises on output results. Chosen threshold in such a way that to reduce errors and improve the accuracy for detection of TB.

$$\text{Threshold} = \left[\frac{Max}{Avg}\right] \min$$

This Threshold value should give minimum error. If the ED<Threshold the test image is non TB image or if the ED>Threshold the test image is non TB image

In this result we used 50 TB Test images are compared with Non-TB Image, threshold value gives 6 images are having error, for 100 TB images error is 12 images. That is out of 100 TB images CBAMI-invariant method decides 12 TB images are not having TB. Hence error is 12 and percentage of Accuracy for CBAMI-invariant method is 88%.

The same process is applied on cavity segmented images Non-TB X-ray image (set1 to set6) and TB X-ray image (SET1 to SET6). The Euclidean Distance (ED) is calculated to detect TB. The Accuracy for detection of TB by using cavity extracted images like Fig.4 e and 4 j is 96%.

CBAMI invariants are calculated from cavity extracted images of Fig. 4 e and 4 j, and Euclidean distance is evaluated. The Euclidean distance is less than threshold value Test image is Non-TB image or if the Euclidean distance is greater than threshold value Test image is TB image. The accuracy is 96%. For comparison, the same experiment is repeated with Geometric moment invariants as features and observed that the accuracy is 88% for entire X-Ray images Figures. a, f. Hence, the CBAMI can be effectively used for extracting features of cavity segmented chest X ray images.

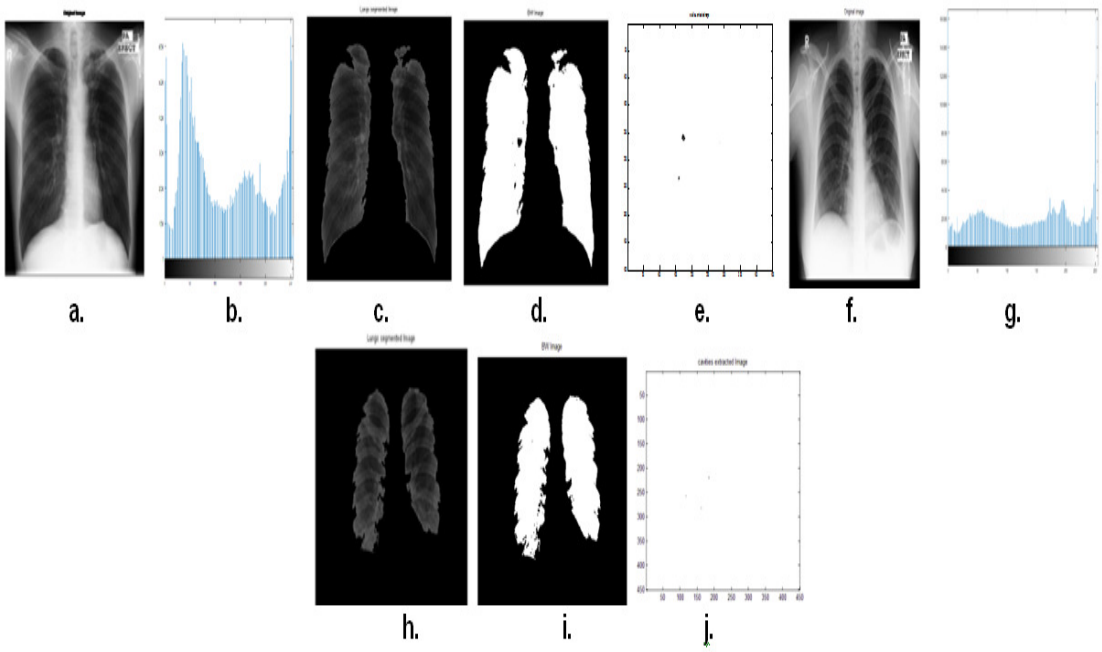


**Fig. 4.** Cavities Extracted from Test (TB Images) Cavities Extracted from Reference (Non-TB) Images. a. Original TB Image, b. Histogram for TB image, c. Lungs Image for TB image, d. BW Image of TB image, e. Cavities in Lungs of TB image, f. Original Non-TB Image, g. Histogram for Non- TB image, h. Lungs segmented image, i. BW image, j. Cavities in Lungs.

Bold values are errors for the detection of TB, The CBAMI method decided that out of 50 TB images two images are non TB images, but these two images are TB images.

CBAMI features are applied on 50 Test Images all these test images are TB Images, but CBAMI detected Image Numbers 15, 38 are non-Tb images. The Images 15, 38 are having Euclidean distance values less than threshold value hence , CBAMI decided these two images are non-TB images. Actually 15 and 38 images are TB images but CBAMI results give wrong detection for two images.

Detection of Tuberculosis using CBAMI as features and Euclidean Distance as classifier applied on cavity extracted images are error is 2 for 50 Test Images and error is 4 for 100 Test Images, so the accuracy is 96%.

**Table 2.**

| S. No | Normal Image (Non-TB Image) figure 4. f | Test Image (TB Image) | Euclidean Distance |
|---|---|---|---|
| 1. | Non-TB Image | Test image 1 | 6.68E+11 |
| 2. | Non-TB Image | Test image 2 | 3.06E+08 |
| 3. | Non-TB Image | Test image 3 | 5.32E+11 |
| 4. | Non-TB Image | Test image 4 | 1.16E+08 |
| 5. | Non-TB Image | Test image 5 | 1.11E+08 |
| 6. | Non-TB Image | Test image 6 | 3.72E+12 |
| 7. | Non-TB Image | Test image 7 | 2.98E+11 |
| 8. | Non-TB Image | Test image 8 | 4.78E+10 |
| 9. | Non-TB Image | Test image 9 | 1.16E+08 |
| 10. | Non-TB Image | Test image 10 | 1.16E+08 |
| 11. | Non-TB Image | Test image 11 | 1.17E+08 |
| 12. | Non-TB Image | Test image 12 | 6.44E+12 |
| 13. | Non-TB Image | Test image 13 | 8.48E+13 |
| 14. | Non-TB Image | Test image 14 | 1.41E+10 |
| 15. | Non-TB Image | Test image 15 | **2.51E+07** |
| 16. | Non-TB Image | Test image 16 | 1.22E+10 |
| 17. | Non-TB Image | Test image 17 | 2.38E+13 |
| 18. | Non-TB Image | Test image 18 | 3.63E+09 |
| 19. | Non-TB Image | Test image 19 | 1.29E+12 |
| 20. | Non-TB Image | Test image 20 | 9.55E+07 |

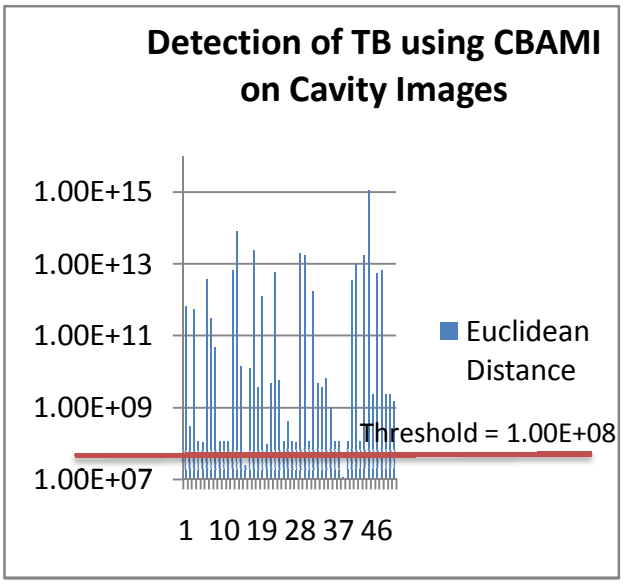


**Fig. 5.** Detection TB using CBAMI on Cavity images.

In the above graph test images are taken on X-axis and Euclidean distance between test and reference images is on Y-axis. The Euclidean distance is less than Threshold value Test image is non TB image and if Euclidean distance is greater than Threshold value Test image is TB image.

## VI. CONCLUSIONS

This paper presented a method for detection of Tuberculosis using CBAMI as features and Euclidean Distance as classifier. The proposed method computes Combined Blur and Affine Moment Invariants (CBAMI) on X-ray image and cavity segmented image and uses them as feature for detection of tuberculosis.

The CBAMI are selected as features in this paper because they are invariant to both affine distortions as well as blur. Hence, the CBAMI can be effectively used for detection of TB from cavity segmented chest X ray images.

## VII. FUTURE SCOPE

CBAMI is based on geometrical moments and is non orthogonal moment invariants, consists of redundant data, hence it is not suitable for reconstruction of X-Ray image from their invariant values. Orthogonal Legendre moments will be used to improve accuracy and reconstruction of Original image from their invariant values.

## REFERENCES


[1]. Rohilla, A., Hooda, R., & Mittal, A. (2017). TB detection in chest radiograph using deep learning architecture. In *Proceeding of 5th International conference on Emerging Trends in Engineering, Technology, Science and Management (ICETETSM-17)* (Vol. 136147).

[2]. P. Quinco, S. B uhrer-Śekula, W. Branddao, R. Monte, S. L. Souza, V. Saraceni, M. Palaci, R. Dietze, and M. Cordeiro-Santos (2013). Increased sensitivity in diagnosis of tuberculosis in hiv-positive patients through the small-membrane-filter method of microscopy," *Journal of clinical microbiology*, vol. **51**, no. 9, pp. 2921–2925, 2013.

[3]. J. Pouchot, A. Grasland, C. Collet, J. Coste, J. M. Esdaile, and P. Vinceneux (1997). Reliability of tuberculin skin test measurement," *Annals of internal medicine*, vol. **126**, no. 3, pp. 210–214.

[4]. Harries, A., Hargreaves, N., Kwanjana, J., & Salaniponi, F. (2001). Clinical diagnosis of smear-negative pulmonary tuberculosis: an audit of diagnostic practice in hospitals in Malawi. *The international journal of tuberculosis and lung disease*, **5**(12), 1143-1147.

[5]. Day, J. H., Charalambous, S., Fielding, K. L., Hayes, R. J., Churchyard, G. J., & Grant, A. D. (2006). Screening for tuberculosis prior to isoniazid preventive therapy among HIV-infected gold miners in South Africa. *The international journal of tuberculosis and lung disease*, **10**(5), 523-529.

[6]. Sivaranjani (2015). Analysis of Tuberculosis in chest using SVM classifier. *National Conference on Research Advances in Communication, Computation, Electrical Sciences and Structures, (NCRACCESS-2015),* 18-21.

[7]. Ankitha B. M., Sanjeev Kubakaddi and Bharathi S. H., (2015). Computer Aided Diagnosis of Tuberculosis using First order Statistical approach", *IPASJ*

*International Journal of Electronics & Communication (IIJEC),* Volume *3*, Issue 4, 22-28.
[8]. Chauhan, A., Chauhan, D., & Rout, C. (2014). Role of gist and phog features in computer-aided diagnosis of tuberculosis without segmentation. *PloS one*, **9**(11), e112980.
[9] Pallavi T. P, Praveen Kumar P. S. (2015). Diagnosis of Tuberculosis by using first order statistics applied to chest radiograph. *International Journal of Sciences & Applied Research, IJSAR,* **2**(8), 16-22.
[10]. Hu. M.K. (1962). Visual Pattern Recognition by Moiments Invariants. IRE Transaction on Information Theory, **8**, 179-187.
[11]. Flusser, J., Suk, T., & Saic, S. (1996). Recognition of blurred images by the method of moments. *IEEE Transactions on Image Processing*, **5**(3), 533-538.
[12]. Tomas Suk and Jan Flusser (2003). Combined Blur and Affine Moment Invariants and their use in Pattern Recognition. *Pattern Recognition***, 36,** 2895 – 2907.
[13]. K. Durga Prasad, M.B.R. Murthy and A. Venkataramana (2017). Diagnosis of Tuberculosis using Combined Blur and Affine Moment Invariants. *International Journal of Advanced Research Trends in Engineering and Technology*, Vol. **4**, Issue 12, 20-25.
[14]. Dai, X., Zhang, H., Liu, T., Shu, H., & Luo, L. (2014). Legendre moment invariants to blur and affine transformation and their use in image recognition. *Pattern Analysis and Applications*, **17**(2), 311-326.
[15]. K. Durga Prasad, M.B.R. Murthy (2019). An improved method for diagnosis of tuberculosis using k-means clustering algorithm and combined blur and affine moment invariants. *Journal of Emerging Technologies and Innovative Research*, Vol. **6** Issue 4, 98-105.
[16]. K. Durga Prasad and M.B.R. Murthy (2019) "Diagnosis of Tuberculosis Using Legendre Moment Invariants". *Journal of Advanced Research in Dynamical and Control Systems,* Vol. **11**, 04-Special Issue, 2219-2226.

**How to cite this article:** Prasad, K. Durga and Murthy M.B.R. (2019). A Method for Diagnosis of Tuberculosis using Combined Blur and Affine Moment Invariants on Cavity Image. *International Journal on Emerging Technologies*, **10**(2): 455–461.